

# 海外招へい校発表

—Invited Presentation—

## Metal Doped Copper Oxide Nanoparticles Modified Electrodes for Determination of Nitrite

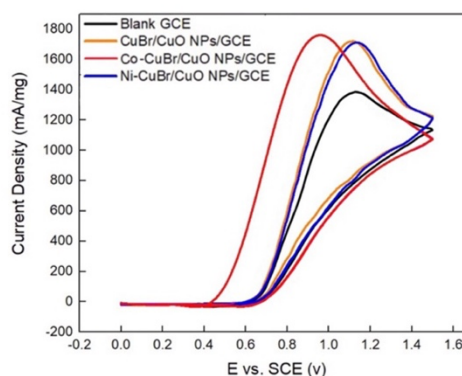
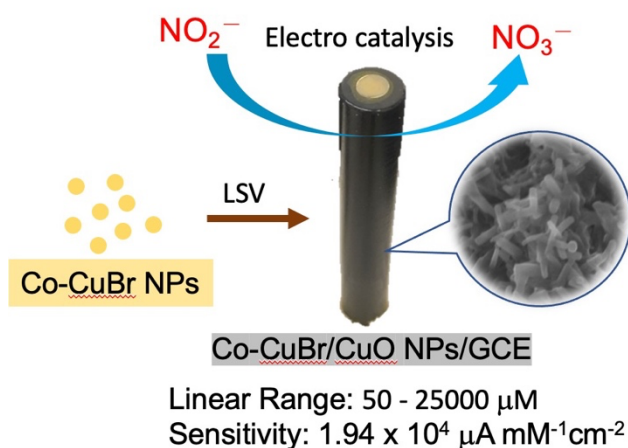
Taipei First Girls High School

Jocelyn Chen

Supervisor : Hwey-Yu Chiang

### Abstract

The occurrence of bacterial infection in the human urine will reduce the nitrate ( $\text{NO}_3^-$ ) to nitrite ( $\text{NO}_2^-$ ), so nitrite can be tested as a routine inspection item for urine. The most common methods for nitrite detection are spectrophotometric detection, chemiluminescence, the voltammetric techniques *etc.* In this study, CuBr/CuO NPs/GCE and metal doped copper oxide NPs electrode (M-CuBr/CuO NPs/GCE, M=Co, Ni) are prepared, and both are electrodes with a nanostructured surface. Co-CuBr/CuO NPs/GCE displays the lower oxidation potential of  $\text{NO}_2^-$  to  $\text{NO}_3^-$  and the better electrocatalytic efficiency in nitrite oxidation. A wide measurement range, 50  $\mu\text{M}$  to 25 mM of  $[\text{NO}_2^-]$ , as well as a good sensitivity,  $1.94 \times 10^4 \mu\text{A mM}^{-1}\text{cm}^{-2}$ , were achieved by using Co-CuBr/CuO NPs/GCE for determination of nitrite. Co-CuBr/CuO NPs/GCE was applied to the nitrite test in an artificial urine, indicating that the sensitivity of  $\text{NO}_2^-$  concentration was  $1 \mu\text{A mM}^{-1}\text{cm}^{-2}$ .



## 1. Introduction

The occurrence of bacterial infection in the human urine will reduce the nitrate ( $\text{NO}_3^-$ ) to nitrite ( $\text{NO}_2^-$ ), so nitrite can be tested as a routine inspection item for urine. The voltammetric techniques are commonly reported for the determination of nitrite. However, the selectivity and the reproducibility are limited to the electrode material as well as structures. Recently the development of nanostructured CuO-based electrode as an efficient electrocatalyst applied on oxidation is very attractive. In this study, we prepare several electrodes with metal doped copper oxide nanoparticles (Ni or Co-CuBr/CuO NPs/GCE) by a simple method and Co-CuBr/CuO NPs/GCE exhibits a good sensitivity as well as reproducibility towards the oxidation of nitrite.

## 2. Experimental Method

### 2.1 Preparation of electrodes with metal doped copper oxide nanoparticles (Co-CuBr/CuO NPs/GCE)

CuBr-NPs were synthesized by mixing 0.1 M  $\text{KBr}_{(\text{aq})}$ , 0.1 M  $\text{CuSO}_{4(\text{aq})}$ , 0.1 M PEG solution with 0.02 M ascorbic acid. After a vigorous stirring, a white suspension was observed. Add 0.1 M  $\text{Co}(\text{CH}_3\text{COO})_{2(\text{aq})}$  into this suspension and let it stay for 10 min. The Co/CuBr-NPs was recovered by a set of repeated centrifugations, and washed several times with distilled water. Drop the Co/CuBr-NPs suspension on the glassy carbon electrode (GCE) and then linear sweep voltammetry (LSV) was used to oxidize the CuBr on the surface of the GCE electrode to CuO in 0.1 M  $\text{NaOH}_{(\text{aq})}$ .

### 2.2 Electrochemical measurements

All electrochemical syntheses and their characterization were performed on CHI 760d electrochemical workstation in a typical three-electrode-cell configuration, with a saturated calomel electrode (SCE) as a reference electrode. The current amperometry (CA) was carried out with a background solution of 0.1 M  $\text{NaOH}_{(\text{aq})}$  and a constant potential of 0.94 V. The cyclic voltammetry (CV) with a potential range of 0~1.5 V and a scan rate of 0.05 V/s was used to compare the oxidation signals of each electrode material to detect  $\text{NaNO}_{2(\text{aq})}$ . The data obtained from the experiment were processed and compared with overlays.

## 3. Results and Discussion

### 3.1 The preparation of CuBr/CuO NPs/GCE and Co-CuBr/CuO NPs/GCE

CuBr NPs on the surface of GCE was converted to CuO by using LSV in 0.1 M NaOH<sub>(aq)</sub>. The SEM image (Fig. 1a) shows CuO NPs deposited on the surface of GCE.

The preparation of Co-CuBr/CuO NPs/GCE is from a cation exchange reaction of M<sup>2+</sup> (M = Co or Ni) with CuBr NPs. After M-CuBr NPs/GCE was oxidized electrochemically by LSV, the nanostructure of M-CuBr/CuO NPs/GCE was observed as shown in Fig 1b. The nanostructured and modified electrode would provide advantages of low overpotential, improved reaction kinetics, and long-term stability toward the electrocatalysis of nitrite oxidation in basic media.

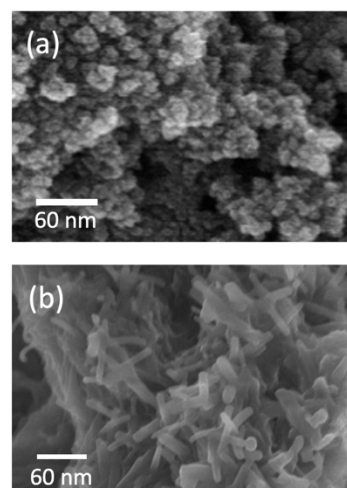


Fig 1. SEM images of (a) CuBr/CuO NPs/GCE (b) Co-CuBr/CuO NPs/GCE

### 3.2 The investigation of the electrocatalytic sensing of nitrite

The electrochemical behavior of bare GCE, CuBr/CuO NPs/GCE, Co-CuBr/CuO NPs/GCE, and Ni-CuBr/CuO NPs/GCE in the presence of 0.1 M NaNO<sub>2(aq)</sub> was studied with a potential of 0.94 V as well as a scan rate of 0.05 V/s in 0.1 M NaOH shown as Fig. 2. The oxidation potentials of NO<sub>2</sub><sup>-</sup> by using bare GCE, CuBr/CuO NPs/GCE, Co-CuBr/CuO NPs/GCE, and Ni-CuBr/CuO NPs/GCE in CV responses were approximately located at 1.13 V, 1.10 V, 0.94 V, and 0.94 V, respectively. (Fig 2) Co-CuBr/CuO NPs/GCE displays better electrocatalytical efficiency in nitrite oxidation.

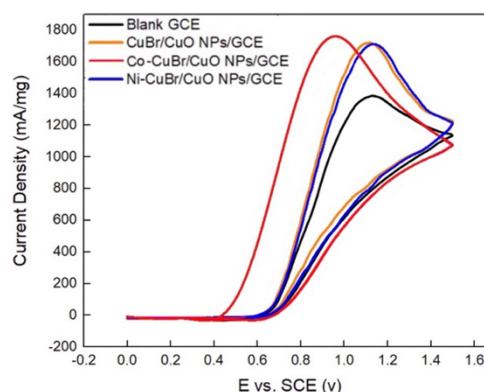


Fig 2. CV graph of modified CuBr/CuO NPs/GCE electrodes in 0.1 M NaNO<sub>2(aq)</sub>

Table 1 Comparison of electrochemical simultaneous response of nitrite at different modified electrodes.

Electrode	Linear Range (μM)	Sensitivity (μA mM <sup>-1</sup> cm <sup>-2</sup> )
CuO-GCE	1 - 91.5	-
CuO-NS / GCE	100 - 1400	6.17
CuBr/CuO-NPs / GCE	-	-
Co-CuBr/CuO NPs/GCE	50 - 25000	19434

The current amperometry (CA) was used to study the sensitivity of the Co-CuBr/CuO NPs/GCE used in nitrite oxidation, the 10  $\mu\text{L}$  0.1 M  $\text{NaNO}_{2(\text{aq})}$  was added every 30 sec to increase the  $\text{NO}_2^-$  concentration. A linear relationship exhibited over the 50 - 25000  $\mu\text{M}$  of  $[\text{NO}_2^-]$  suggested a wide measurement range as well as a good sensitivity,  $1.94 \times 10^4$   $\mu\text{A mM}^{-1}\text{cm}^{-2}$ . (Table 1) The presence of interferences, such as NaCl, uric acid, ascorbic acid, and  $\text{Na}_2\text{SO}_3$ , do not influence the detection of nitrite. (Fig. 3)

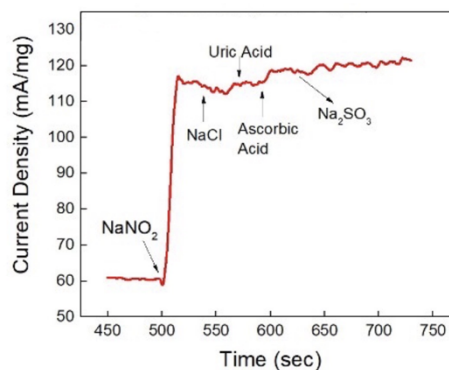


Fig 3. The interference test of the different adducts for nitrite determination. (Electrode: Co-CuBr/CuO NPs/GCE, 1.0 M 10  $\mu\text{L}$   $\text{NaNO}_{2(\text{aq})}$  in 0.1 M NaOH, Adduct : 0.1 M 10  $\mu\text{L}$ )

Because urinary tract infections are the most common cause of nitrites in urine, Co-CuBr/CuO NPs/GCE was applied to the nitrite test in an artificial urine containing  $\text{CaCl}_2$ ,  $\text{NH}_4\text{Cl}$ ,  $\text{MgSO}_4$ , NaCl, KCl, uric acid, ascorbic acid, sodium citrate, urine, or  $\text{Na}_2\text{SO}_4$ . The sensitivity of  $\text{NO}_2^-$  concentration was 1  $\mu\text{M}$  in the nitrite test in the artificial urine.

#### 4. Conclusion and Future View

In summary, CuBr/CuO NPs/GCE and Co-CuBr/CuO NPs/GCE are prepared by using linear voltammetry (LSV) in 0.1 M  $\text{NaOH}_{(\text{aq})}$  of CuBr NPs/GCE and Co-CuBr NPs/GCE, and both are electrodes with a nanostructured surface. Co-CuBr/CuO NPs/GCE displays the lower oxidation potential of  $\text{NO}_2^-$  to  $\text{NO}_3^-$  and the better electrocatalytical efficiency in nitrite oxidation. A wide measurement range, 50  $\mu\text{M}$  to 25000  $\mu\text{M}$  of  $[\text{NO}_2^-]$ , as well as a good sensitivity,  $1.94 \times 10^4$   $\mu\text{A mM}^{-1}\text{cm}^{-2}$ , were achieved by using Co-CuBr/CuO NPs/GCE for determination of nitrite. Co-CuBr/CuO NPs/GCE was applied to the nitrite test in an artificial urine, showing that the sensitivity of  $\text{NO}_2^-$  concentration was 1  $\mu\text{A mM}^{-1}\text{cm}^{-2}$ .

In the future, the performance of Co-CuBr/CuO NPs/GCE would be investigated in detection of other harmful ions and food additives.

#### 6. References

- [1] Casella, I. G.; Gatta, M. *Journal of Electroanalytical Chemistry* **2004**, 568, 183-188.
- [2] Sudha, V.; Krishnamoorthy, K.; Senthil Kumar, S. M.; Thangamuthu, R. *Journal of Alloys and Compounds*, **2018**, 764, 959-968.
- [3] Wu, C.-W.; Unnikrishnan, B.; Periasamy, A. P.; Chen, I. W. P.; Tseng, Y.-T.; Yang, Y.-Y.; Lin, W.-J.; Huang, C.-C.; Chang, H.-T. *ACS Sustainable Chemistry & Engineering*, **2020**, 8 (26), 9794-9802.



## 1. Introduction

Sound is a mechanical wave which travels through the vibration of particles of the medium. When sound vibrations are applied to a fluid from the bottom, the standing wave patterns formed on the surface of a vertically oscillated fluid enclosed by a container. The modes are a spatial and a temporal patterning. In this study, we successfully demonstrate a reaction–diffusion system that produces Chladni Pattern induced by a self-design audible sound-controlled system. The reaction–diffusion system is based on a redox-sensitive chemistry of blue bottle reaction or a pH-sensitive chemistry of acid–base indicators.

## 2. Experimental

### 2.1 Faraday wave and Chladni Pattern

Faraday waves are nonlinear standing waves (Fig. 1) which formed on the surface of a vertically oscillated fluid enclosed by a container have long been a subject of fascination. In circular containers, stable and radially symmetrical Faraday wave patterns are resonant phenomena, and occur at the vibrational modes where whole numbers of waves fit exactly onto the surface of the fluid sample.

With standing waves on two-dimensional membranes, the nodes become nodal lines, lines on the surface at which there is no movement, that separate regions vibrating with opposite phase. These nodal line patterns are called Chladni patterns. (Fig. 2)

### 2.2 Blue bottle reaction

In the presence of oxygen or air, 3 drops of methylene blue (MB) solution were added into a mixture of 1.0 M glucose 8 mL and 1.0 M NaOH solution 2 mL. Allow to stand and the blue color in the container slowly disappears forming a colorless solution. If the container is shaken a few times, then the blue color is restored. This cycle of color change can be repeated many times.

### 2.3 Sound-controlled spatiotemporal patterns

Blue bottle reaction solution was kept in a grand container with an inner diameter of 35.0 mm in which the height of the solution remained 5.0 mm at room temperature in the presence of oxygen or air. Put this solution undisturbed in a container on the vibrating plate of a self-design sound-controlled system. Patterns generated when sound was applied.

## 3. Results and Discussion

### 3.1 The Chladni patterns in blue bottle reaction

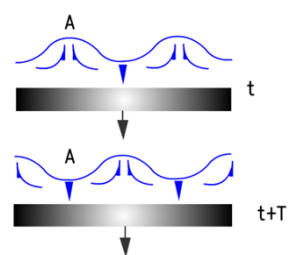


Fig. 1 Schematic diagram of Faraday waves

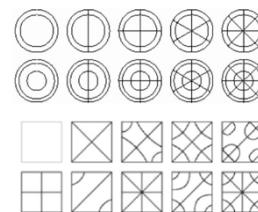
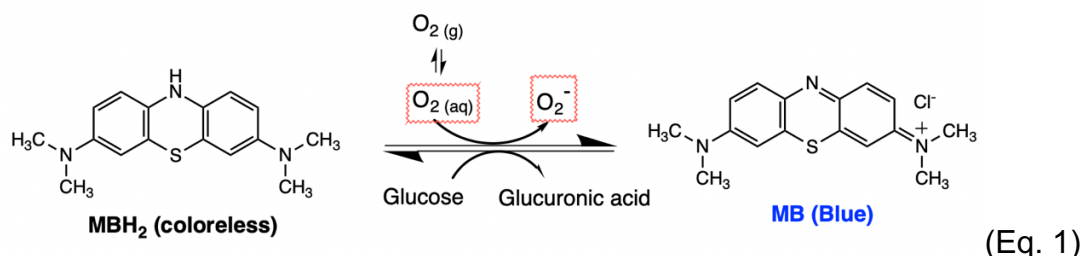


Fig. 2 Chladni patterns on a round plate and a square plate.

Blue bottle reaction is a redox reaction by using methylene blue (MB) as an indicator. An alkaline solution of glucose acts as a reducing agent and reduces MB from a blue to a colorless form, MBH<sub>2</sub>. Then the oxygen dissolved in the mixture oxidizes the MBH<sub>2</sub> back to its blue form, MB. (Eq. 1) When the dissolved oxygen has been consumed, the MB is slowly reduced back to its colorless MBH<sub>2</sub> by the remaining glucose, and the cycle can be repeated many times.



Put the undisturbed blue bottle reaction mixture in a container on the vibrating plate of a self-design sound-controlled system and exposed to air, vibrated the solution, and then the intense blue solution gradually reorganized into a pattern. The spatiotemporal patterns exhibited a 'self-healing' property that restored the original pattern structure after being manually disturbed. The formation of patterns is influenced by frequency, amplitude as well as the container size including internal diameter and the depth. Clear Chladni Patterns are observed with a sound source operating at a specific frequency which results from the vibrated vertically by resonant driving frequency. (Table 1)

Table 1 Frequency-dependent Chladni pattern in blue bottle reaction.

The Shape of container	Round				Square			
	0	8	28	48	31	35	38	41
Frequency (Hz)								
Experimental Photograph								
Chladni pattern								

When the shape of container is ground, the pattern shows subsequent refuelled cycles consisting of concentric vertically aligned blue and colorless rings. At high-blue regions, antinodes of the standing wave, the vertical vibration of the sound had a larger amplitude, which promotes oxygen in the air to dissolve into the solution where the color becomes blue in presence of MB. On the opposite, at zero-blue regions (nodes) colorless reduced form, MBH<sub>2</sub>, was the main species because of a steady supply presence of reducing agent, glucose.

Blue bottle variation in concentration in Chladni Patterns was obtained from the

cross-sectional study through RGB absorbance. (Fig. 3) In the central region of circle ( $n = 0$ ), the concentration of MB is  $1.52 \times 10^{-4} \text{ M}$ , which is 1.55 times higher than other high-blue regions ( $n = 1, 2, 3$ ),  $9.75 \times 10^{-5} \text{ M}$ .

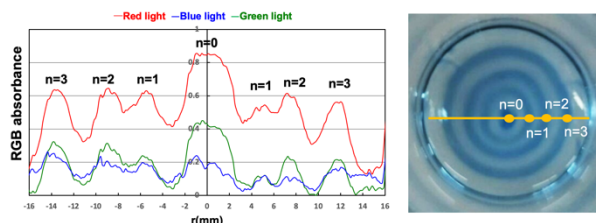


Fig. 3 The spatial - RGB absorbance spectrum of blue bottle reaction during Chladni patterns generation.

### 3.2 The patterns in acid-base system

Next, we controlled the dissolution and diffusion of  $\text{CO}_2$  in to an alkaline solution in which a universal indicator or Phenolphthalein is used as indicator by using sound. The patterns in an acid-base system were shown in Fig. 4. When an alkaline solution under  $\text{CO}_2$  atmosphere is placed on a vertical vibrating plate, driven by resonant frequency, the antinodes of the standing wave will turn to be acidic owing to more  $\text{CO}_2$  dissolved by larger amplitude.

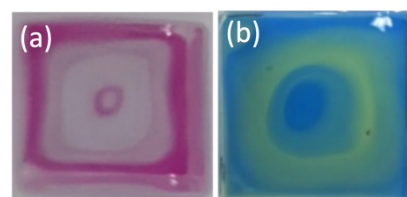


Fig. 4 The patterns in an acid-base system using (a) Phenolphthalein or (b) universal indicator as indicator.

## 4. Conclusions and Future Research

In summary, we successfully demonstrate a reaction–diffusion system that produces Chladni Pattern induced by a self-design audible sound-controlled system. The reaction–diffusion system is based on a redox-sensitive chemistry of blue bottle reaction or a pH-sensitive chemistry of acid–base indicators. Vertical vibrations can control the dissolution of atmospheric gases ( $\text{O}_2$  or  $\text{CO}_2$ ) in water and segregate the solution into spatiotemporal domains corresponding to different redox states or pH values to generate Chladni patterns in the bulk of the blue bottle solution or acid-base system. Blue bottle variation in concentration in Chladni Patterns was obtained from the cross-sectional study through RGB absorbance.

In the future, we wish to investigate other chemical systems, the mechanism as well as fluid dynamics of the formation of sound-controlled spatiotemporal patterns. This approach would be utilized to biology, for instance, the formation of biofilm and the development of acoustofluidic devices.

## 5. References

- [1] Hwang, I., Mukhopadhyay, R. D., Dhasaiyan, P., Choi, S., Kim, S. -Y., Ko, Y. H., Baek, K., Kim, K. *Nature Chemistry*, **2020**, *12*, 808
- [2] Lehar, S., *Perception*, **2003**, *32*, 423 – 448.
- [3] Hong, S.-H., Gorce, J. -B., Punzmann, H., Francois, N., Shats, M., Xia, H. *Sci. Adv.* **2020**, *6*: eaaz9386.

Chalcone-ligated molybdenum carbonyl complexes:  
Synthesis and evaluation as quadruplex DNA binders

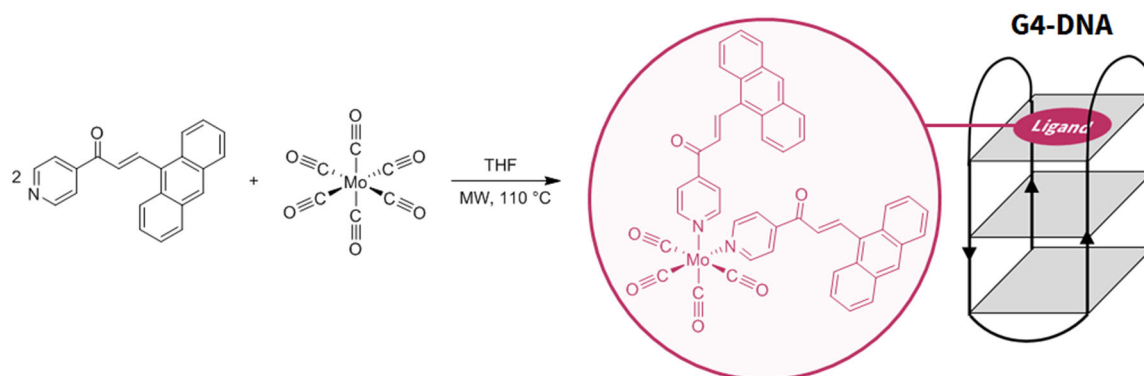
Hwa Chong Institution, Singapore

Lim Kar Ern Samuel, Ang Kang Yu Daniel

Supervisor: Dr Tan Yong Leng Kelvin

**Abstract**

The microwave-assisted reaction of  $\text{Mo}(\text{CO})_6$  with isomeric pyridyl anthryl chalcones **1a-f** afforded six novel molybdenum carbonyl complexes **2a-f**. Complexes **2a-f** have been characterized by infrared and  $^1\text{H}$  Nuclear Magnetic Resonance spectroscopies, and the structures of **2a-d** were revealed to be *cis*-disubstituted complexes with general formula  $\text{Mo}(\text{CO})_4\text{L}_2$ . The intercalative abilities of **2a-d** towards quadruplex DNA were examined using the Fluorescent Intercalator Displacement (FID) assay.



## 1. Introduction

Recently, a structure known as the G-quadruplex (G4) has emerged as a promising anti-cancer drug target. G4 structures are helical structures formed in guanine-rich regions of RNA or DNA sequences stabilised by sodium or potassium cations [1]. Such structures are found in higher frequency in telomeres and promoters [2], suggesting that they may play a role in cancer regulation. It is hence hypothesised that molecules that can stabilise G4 structures may display anti-cancer activity.

Chalcones are a class of plant secondary metabolites featuring the  $\alpha,\beta$ -unsaturated ketone pharmacophore and display a wide range of biological activity [3]. Pyridyl anthryl chalcones contain the planar anthryl group, which has a large  $\pi$  surface area, potentially allowing it to intercalate between the guanine bases and act as a ligand for G4 structures, enhancing its anti-cancer activity. On the other hand, molybdenum carbonyl complexes have been investigated as Carbon Monoxide Releasing Molecules (CORMs) which can release therapeutic amounts of carbon monoxide to tissues [4]. The attachment of pyridine anthryl chalcones to molybdenum carbonyl complexes may enhance its G4-binding ability due to electrostatic attraction between the metal center and the negatively-charged phosphate backbone of the G4-DNA.

In this work, molybdenum carbonyl complexes **2a-f** were synthesised by the reaction of  $\text{Mo}(\text{CO})_6$  with the anthryl pyridine chalcones **1a-f** (Chart 1). The intercalative abilities of **2a-d** towards quadruplex DNA were examined to ascertain their potential as anti-cancer agents.

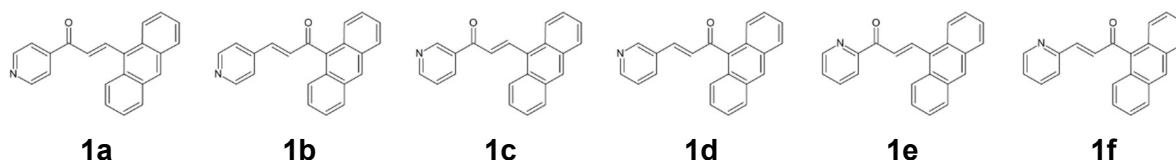


**Chart 1.** Structures of **1a-f**

## 2. Experimental

### *Synthesis of molybdenum complexes 2a-f*

$\text{Mo}(\text{CO})_6$  (15 mg, 57  $\mu\text{mol}$ ) and the corresponding chalcone (2 molar equivalent) were added to 1 mL of tetrahydrofuran and reacted in a Discover-SP microwave reactor. The solvent was removed under reduced pressure and the residue was washed with hexane and air dried to yield the solid product.

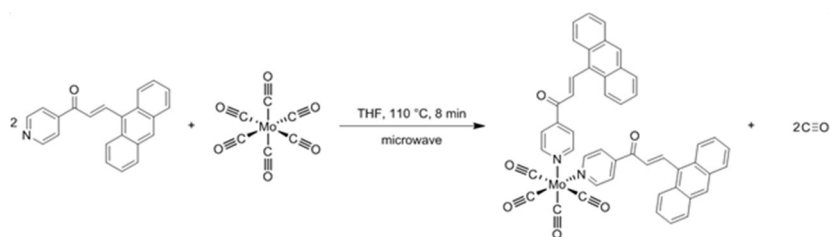
### *Fluorescent Intercalator Displacement (FID) assay*

The FID assay [5] was performed on **2a–d** against G4 quadruplex DNA (HTelo and *c-myc*) as well as duplex DNA (ds26) to obtain their corresponding half-maximal degradation concentration ( $DC_{50}$ ) values.

### 3. Results and Discussion

#### Synthesis and characterization

The reaction of  $Mo(CO)_6$  with the respective chalcone **1a–d** afforded the novel *cis*-disubstituted molybdenum carbonyl complexes **2a–d** (Scheme 1) in moderate yields. All complexes were characterised by infrared (IR) and  $^1H$  Nuclear Magnetic Resonance (NMR) spectroscopies.



**Scheme 1.** Synthesis of the *cis*-disubstituted complex **2a**

The IR spectra of **2a–d** in the  $\nu_{CO}$  region (Figure 1) resembles those of previously reported *cis*- $Mo(CO)_4(\text{amine})_2$  complexes [6], confirming the identities of **2a–d**.

The  $^1H$  NMR spectra of all complexes displayed one set of signals, suggesting that the complexes are symmetrical in solution. The assignment of protons on **2a** (Figure 2) is used as an example. The singlet at  $\delta = 8.51$  ppm can be assigned to the proton on position 10 on the anthracene ring, while the doublet at  $\delta = 8.87$  ppm can be assigned to the protons at the *ortho* position of the pyridine ring. The two sets of doublets at  $\delta = 8.87$  ppm and  $\delta = 7.54$  ppm with coupling constant  $J = 16.0$  Hz can be assigned to the vinylic protons. The value of the coupling constant suggests that the chalcone exists in the *trans* configuration.

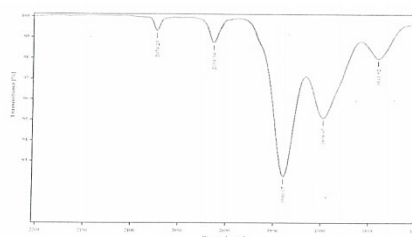


**Figure 1.** IR spectrum of **2a** in dichloromethane solution

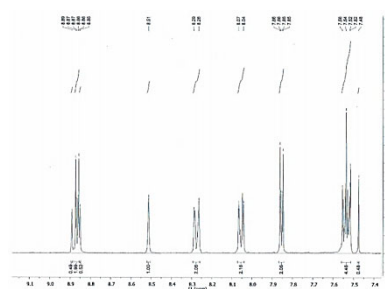


**Figure 2.**  $^1H$  NMR spectrum of **2a** in  $CDCl_3$

#### Fluorescent Intercalator Displacement (FID) Assay

The  $DC_{50}$  values of **2a–d** were determined using the FID assay (Table 1); a lower  $DC_{50}$  value is indicative of better quadruplex intercalative properties.

While  $Mo(CO)_6$  and **1a–d** did not bind to quadruplex DNA, complexes **2a–d** were able to intercalate to HTelo and *c-myc*. This suggests that there might be synergistic effects, such as

electrostatic attraction, which allow **2a-d** to intercalate. All four complexes showed greater selectivity for HTelo over *c-myc*. This might be because *c-myc* adopts a parallel topology while HTelo forms a (3+1) hybrid, and the more compact structure of *c-myc* would increase the difficulty of intercalation. However, all complexes showed

greatest selectivity for duplex DNA, suggesting an alternative mode of interaction besides intercalation.

#### 4. Conclusion

Six novel molybdenum carbonyl complexes with chalcone ligands were synthesized and characterized. FID assays revealed that **2a-d** displayed moderate intercalative abilities for quadruplex DNA while having greater selectivity for HTelo over *c-myc*.

#### 5. Future Work

The identities of **2e** and **2f** will be established followed by FID assays on these two complexes, and the brine shrimp lethality (BLT) assay will be carried out on complexes **2a-f** to evaluate their cytotoxicity.

#### 6. References

- [1] Howard, F. B.; Frazier, J.; Miles, H. T. *Biopolymers* **1977**, *16* (4), 791.
- [2] Chambers, V. S.; Marsico, G.; Boutell, J. M.; Di Antonio, M.; Smith, G. P.; Balasubramanian, S. *Nat. Biotechnol.* **2015**, *33* (8), 877.
- [3] K. Sahu, N.; S. Balbhadra, S.; Choudhary, J.; V. Kohli, D. *Curr. Med. Chem.* **2012**, *19* (2), 209.
- [4] Kromer, L.; Coelho, A. C.; Bento, I.; Marques, A. R.; Romão, C. C. *J. Organomet. Chem.* **2014**, *760*, 89.
- [5] Monchaud, D.; Allain, C.; Teulade-Fichou, M.-P. *Bioorg. Med. Chem. Lett.* **2006**, *16* (18), 4842.
- [6] Kraihanzel, C. S.; Cotton, F. A. *Inorg. Chem.* **1963**, *2* (3), 533.

Compound	DC <sub>50</sub> <sup>a</sup> / μM		
	HTelo	<i>c-myc</i>	ds26
<b>2a</b>	44.33 (2.29)	54.33 (1.82)	10.01 (0.18)
<b>2b</b>	39.87 (0.31)	74.77 (0.51)	9.03 (0.09)
<b>2c</b>	55.87 (1.22)	81.85 (3.03)	10.71 (0.34)
<b>2d</b>	39.20 (0.37)	102.88 (4.14)	10.35 (0.21)

<sup>a</sup> Standard errors (*N* = 3) are shown in parentheses.

**Table 1.** Affinity and selectivity of **2a-d** for oligonucleotides, determined by the FID assay